---

**Article:**
Santa, J.F., Cuervo, P., Christoforou, P. orcid.org/0000-0001-8547-4878 et al. (4 more authors) (2019) Twin disc assessment of wear regime transitions and rolling contact fatigue in R400HT – E8 pairs. Wear, 432-433. 102916. ISSN 0043-1648

https://doi.org/10.1016/j.wear.2019.05.031

---

# TWIN DISC ASSESSMENT OF WEAR REGIME TRANSITIONS AND ROLLING CONTACT FATIGUE IN R400HT – E8 PAIRS

**J.F. Santa[1,3], P. Cuervo[1*], P. Christoforou[2], M. Harmon[2], A. Beagles[2], A. Toro[1], R. Lewis[2]**

[1] Tribology and Surfaces Group, Universidad Nacional de Colombia, Medellín, Colombia

[2] Department of Mechanical Engineering, University of Sheffield, UK

[3]Grupo de Investigación Materiales Avanzados y Energía – MATyER. Instituto Tecnológico Metropolitano,

**Abstract**: Twin disc tests were carried out to evaluate the wear resistance and Rolling Contact Fatigue (RCF) of premium R400HT rail samples in contact with E8 wheel samples. The wear rate and friction coefficient were correlated with the frictional work expended at the contact interface (the Tgamma approach). Accelerated RCF tests were also carried out on the premium R400HT rail and the results were compared to those obtained for standard R260 rail. The wear rates of rail samples were consistently lower than those reported in the literature for other contacting pairs in which the rail material studied is softer than R400HT. Also, the energy needed for the transition from the moderate to severe wear regime significantly increased for the hardened rail. Fatigue cracks were shallower for R400HT when compared with standard rail material. Hardened rails also showed lower mean spacing between fatigue cracks. This new information can be used to improve wear simulations of wheels and rails by using more realistic wear equations.

**Keywords**: Twin disc testing; Premium rail; Tgamma approach; Wear rate; Rolling contact fatigue.

## 1. INTRODUCTION

This paper outlines a study of the wear and fatigue behaviour of specimens extracted from wheels and rails of the commercial railway system of the Metro de Medellín in Colombia. The materials were subjected to controlled rolling-sliding conditions using twin-disc testing machines.

Wheel and rail materials play a very important role in the optimization of the management of wheel-rail

contacts. The choice of rail material, for example, can determine whether wear or fatigue processes are dominant. Therefore, studying the tribological behaviour of a pair of materials under diverse contact conditions is key to understanding the transitions between different wear regimes. Hiensch and Steenbergen [1], for instance, used data from the field to show that premium R370CrHT grade rail offers better resistance to Rolling Contact Fatigue (RCF) than conventional R260Mn grade, mainly because the wear number (Tgamma) associated with fatigue crack initiation for the harder rail is higher. They note that quantitative determination of the wear and RCF behaviour of the steels in the descending part of the damage function could be found using twin-disc testing; an approach that we describe here.

Laboratory studies have also been carried out to identify wear transitions in materials for wheels [2,3] and rails [4-7]. Pin-on-disc, twin-disc, and full-scale rigs have been used for this and there has been some successes in transferring the results from the laboratory to the field. Pioneer works from Danks and Clayton [8], McEwen and Harvey [9] and Bolton and Clayton [10] allowed correlations between laboratory tests and field data to be established for specific operation conditions. Basic theoretical models to predict wear of rails in service were proposed. Ma et al [11] tested ER9 wheel – U71Mn rail pairs in a twin disc machine with slip ratios from 0.17% to 9.43% and found that the transition from mild to severe wear regime occurred at a slip ratio of about 3.8%. The transition was also linked to changes in the main mechanisms of damage of the contact surfaces. In the mild regime the cracks propagated mainly parallel to the contact surface, while in severe regime the angle with respect to the surface increased and detachment of material from the surface became more frequent. The Tgamma approach has been implemented to model the behaviour of materials as a function of the contact conditions. According to this approach [12], it is assumed that the wear rate (mass lost per mm² of surface area per m that the interface slides) is related to the frictional work done at the wheel/rail contact, i.e. to the amount of energy available at the contact interface.

On the other hand, Rolling Contact Fatigue (RCF) is a common failure mechanism in rails [13]. Typical testing of RCF has been done by performing dry twin disc tests up to 800.000 cycles and monitoring the damage with the aid of an accelerometer. However, those tests are expensive and time consuming.

Kaneta and Murakami [14] studied experimentally the effects of oil pressure on surface crack growth in rolling-sliding contacts by using transparent polycarbonate resin discs in a twin disc machine and they found that hydraulic pressure applied repeatedly on the crack face induces fatigue crack growth. Bower [15] reported on experimental work that had found that: i) cracks will propagate only if a fluid is applied to the surfaces in contact, ii) cracks always grow in the loading direction over the surface, and iii) if sliding occurs, the cracks will grow only in the driven surface. He developed a two-dimensional model of wheel/rail contact and explored the effect of fluids on crack propagation mechanisms. It is clear that fluid can be used to accelerate RCF tests in the laboratory compared to dry tests.

A short survey of different articles studying rolling contact fatigue was undertaken to identify different testing techniques. Several methods have been developed to study RCF including those by Kaneta and Murakami, [14], Tyfour, Beynon, and Kapoor [16], Fletcher and Beynon, [17], Liu, Jiang and Magel [18], Stock and Pippan [19], and Eadie et al. [20]. Three different types of tests were identified [21]: 1. Accelerated tests [17,18], 2. Long-term tests [18,20] and 3. Full-Scale-Rig tests [19,20]. Approach (1) was chosen here because it offers the possibility of acquiring large amounts of quantitative data in short periods of time and allows studying the effects of individual variables on the tribological response of the wheel-rail pairs.

This work presents the results of twin-disc tests carried out with samples extracted from E8 wheels and premium R400HT rails. The purpose of the experiments was to identify the wear regime transitions and to compare the behaviour of the premium rail with that of softer materials already reported in the literature. In addition, accelerated Rolling Contact Fatigue (RCF) tests were done to evaluate typical rail materials (R260 and R350HT) to compare with the behaviour of premium R400HT rails.

## 2. MATERIALS AND METHODS

### 2.1 Samples preparation

Cylindrical specimens were extracted from wheels and rails that had been in service on the Medellín metro by cutting and lathe turning. The rail specimens were extracted from the rail head as shown in **Fig. 1**. Both rail and wheel specimens had a diameter of 47 mm and the width of the contact zone was 10 mm. For Tgamma tests only hardened premium R400HT rail samples were used. For Rolling Contact Fatigue tests, R260 and R350HT rail samples were also studied. All rail materials were tested in contact with standard wheel material (E8). These designations are covered by standards EN 13674-1 (rails) and EN 13262 (wheels). The chemical composition of the materials used in this work, measured by optical emission spectroscopy (OES), is shown in **Table 1.**

**Table 1.** Chemical composition of rail and wheel samples (wt.%)

| | C | Si | Mn | P | S | Cr | Al | V | Cu | Ti | Ni | Mo |
|---|---|---|---|---|---|---|---|---|---|---|---|---|
| **R260** | 0.736 | 0.270 | 1.056 | 0.032 | 0.023 | 0.026 | | 0.003 | 0.002 | 0.016 | 0.021 | 0.006 |
| **R350HT** | 0.739 | 0.453 | 1.198 | 0.016 | 0.013 | 0.085 | - | 0.001 | | | | |
| **R400HT** | 0.931 | 0.251 | 1.269 | 0.009 | 0.022 | 0.275 | - | 0.0035 | 0.017 | 0.002 | 0.015 | 0.0068 |
| **E8** | 0.542 | 0.253 | 0.734 | 0.011 | 0.006 | 0.141 | 0.027 | 0.006 | 0.165 | 0.002 | 0.120 | 0.048 |

### 2.2 Assessment of wear regime transitions

Twin disc tests were performed at the National University of Colombia and at the University of Sheffield, UK under identical conditions. The average results of the tests are shown in this work while the reliability of inter-laboratory testing as well as its limitations for practical purposes are discussed elsewhere [21]. All the tests were conducted in dry condition with 1300 MPa contact pressure and 400 RPM rotational speed. The tangential force between the discs was measured during the tests to correlate the wear rates with the energy dissipated in the contact by unit volume (Tgamma/A approach). Ten different slip ratios varying from 0 to 20% were used. Four tests were performed for each slip value.

### 2.3 Rolling Contact Fatigue (RCF) testing

R260, R350HT and R400HT rail materials were tested under Rolling Contact Fatigue (RCF). The main purpose of the tests was to contribute to the understanding of the fatigue behaviour of hardened premium rail R400HT in contrast with that of softer rails. This characteristic of the R400HT was of special interest

for Metro de Medellín since routine inspections in the field revealed the nucleation of cracks at the surface of the rails just a few months after installation, with an accumulated traffic of circa 8 MGT (million gross tons) [23]. It is expected that this work can contribute to understand some aspects of the behaviour of R400HT rail grade under RCF and to either confirm or rule out possible material issues responsible for the observed lack of performance in the field.

The rolling contact fatigue tests were performed on a SUROS machine [21] using 1% creepage and a maximum contact pressure of 1300 MPa. An initial experiment consisted in running a fixed number of dry cycles (8000), a methodology that has been used before [23, 24]. After the tests, the samples were cut as shown in **Fig. 1b**, polished and chemically etched to measure the thickness and microhardness ($HV_{100g,\ 10\ s}$) of the strain-hardened layer formed as a result of the contact conditions.

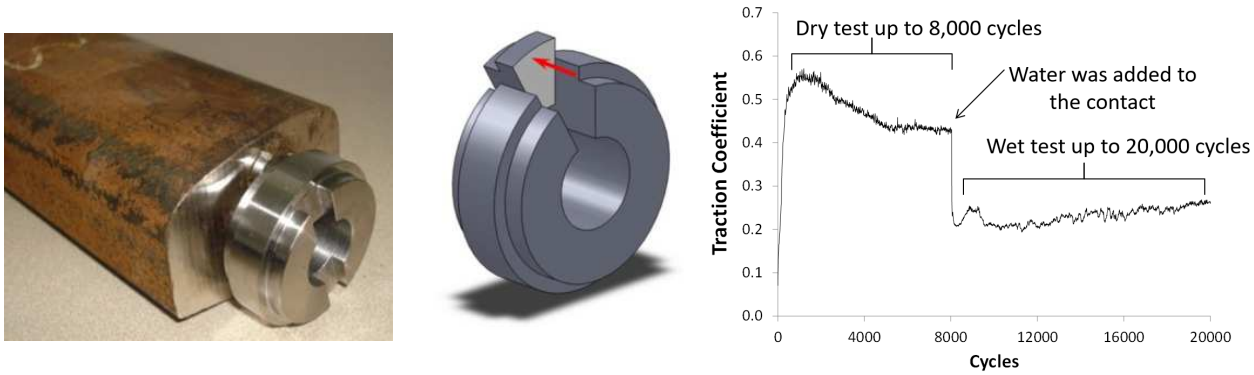


a) b) c)

***Figure 1.*** *Details of samples and twin disc testing conditions. a) Extraction of a sample from the rail head, b) Sectioning of a sample to examine the deformed layer and the cracks formed during the tests, c) Typical variation of friction in dry and wet conditions.*

A second experiment consisted of running the same number of dry cycles (8000) to accumulate surface fatigue, and then adding 0.125 g per second of deionized water to the contact zone for 12000 cycles (for a total of 20 thousand cycles) as shown in **Fig. 1c**. At the end of the tests, the wear rates of different materials were compared. Two repeats for each material were performed and after the tests the crack

parameters (mean spacing, angle with respect to the surface, and depth) were measured. The worn surfaces were also observed in Stereoscopic (SM) and Scanning Electron (SEM) microscopes.

## 3. RESULTS AND DISCUSSION

### 3.1. Wear regime transitions

**Fig. 2** shows the wear rate of wheel and rail samples plotted against the wear index Tgamma/A, where T refers to the tangential force at the contact interface in newton, gamma (γ) is the dimensionless slip ratio, and A is the contact area in mm². The wear rate for the wheel sample was about one order of magnitude higher than that for the rail sample for a wide range of slip values. A linear relationship between wear rate and wear index was observed for wear indices below 25 N/mm² while no clear dependence of the wear rate on the wear index was seen for wear indices between 25 and 80 N/mm². When the slip ratio was increased to 20%, Tγ/A reached about 90 N/mm² and the wear rate of the rail sample tripled, which indicates that a transition from a severe to a catastrophic wear regime had occurred.

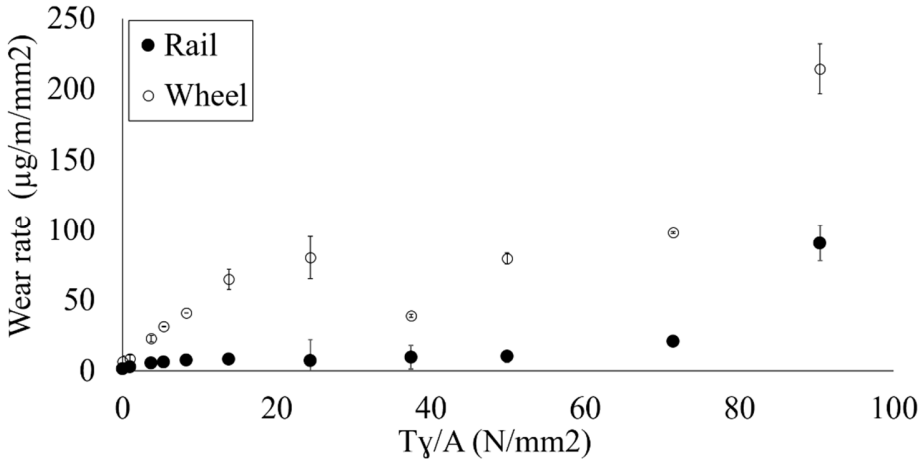


***Figure 2.*** *Average wear rates for R400HT rails rolling-sliding against E8 wheels for different slip ratios from 0 to 20%*

A close-up of the Tgamma curve for wear indices between 0 and 25 N/mm² is shown in **Fig. 3**, where two features become evident: a) for low slip values, a linear relationship between the wear rate and the wear index Tγ/A can be established for both wheel and rail samples, and b) different Tγ/A thresholds can be defined for the wheel and rail samples to mark the end of the linearly dependent region; this agrees with previous reports by Lewis & Olofsson [2]. The wear rate of the rail samples did not exceed 100 μg/(m.mm²) even under the very harsh conditions imposed using a slip ratio of 20%. On the other hand, under such aggressive conditions, the wear rate of the wheel samples significantly increased, as did the magnitude of the surface damage observed at the end of the tests.

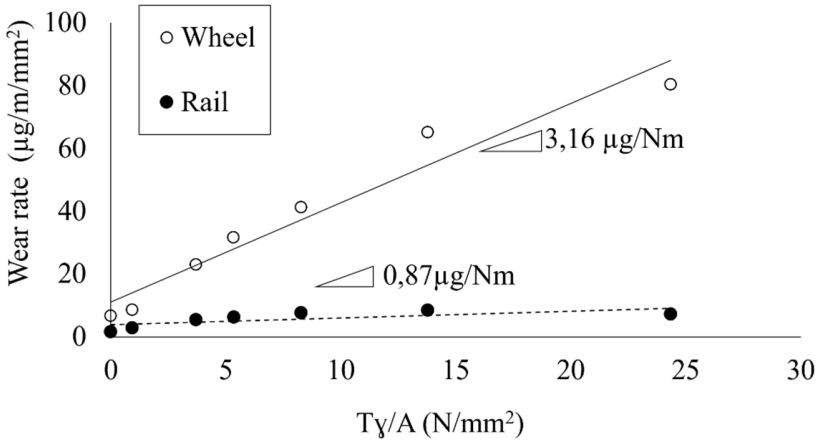


***Figure 3.*** *Wear rate for R400HT rail samples rolling-sliding against E8 wheel samples for wear indexes lower than 25 N/mm².*

**Fig. 4** shows the COF and the wear rates of wheel and rail samples versus the percentage of slip. The COF initially increases with slip ratio, and then stabilizes around a value of 0.5 for slip ratios higher than about 7%. For very high slip percentages there is a slight decrease in COF; a value of 0.4 was measured in the tests performed with a slip of 20%.

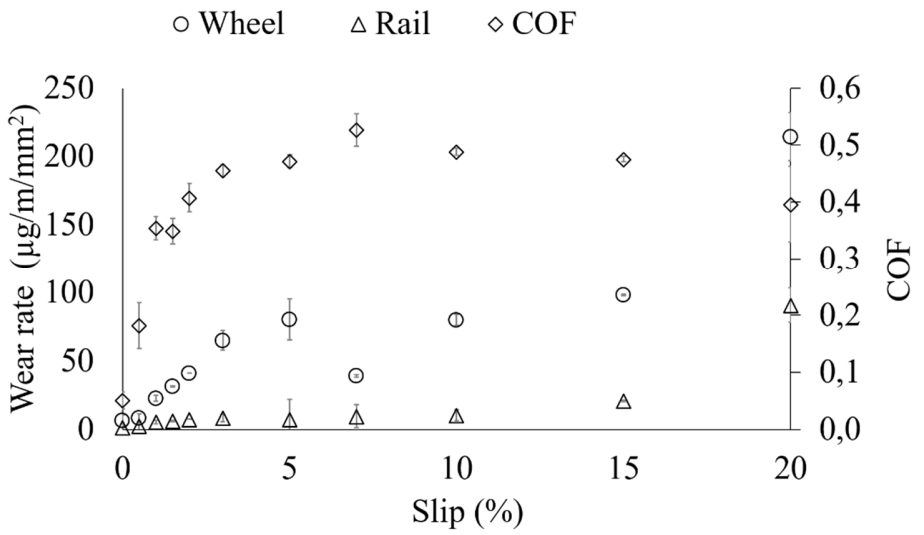


***Figure 4**. COF and wear rates versus slip ratio for R400HT rail samples in contact with E8 wheel samples for different slip ratios.*

**Fig. 5** compares the wear rates of R400HT rail (a) and wheel E8 (b) tested in this work with those reported in the literature for other rail and wheel materials [2,3,7-9,10,13]. The wear rates for the R400HT-E8 pair are significantly lower than those found in other pairs for virtually all the Tγ/A values studied. Comparison with the results reported in the literature after tests with Class D wheel material are of special interest since this steel has hardness and microstructure similar to the E8 steel studied in this investigation, so the differences in the behaviour of the pairs can be associated mostly with the characteristics of the rail materials. It is worth noticing that the measured wear rates for R400HT rail samples were always below 50 µg/(m.mm²) regardless of the value of Tγ/A, with the sole exception of the case when Tγ/A was extremely high, about 90 N/mm², while the BS11 rail material, for instance, shows wear rates higher than 50 µg/(m.mm²) even for Tγ/A values as low as 10 N/mm².

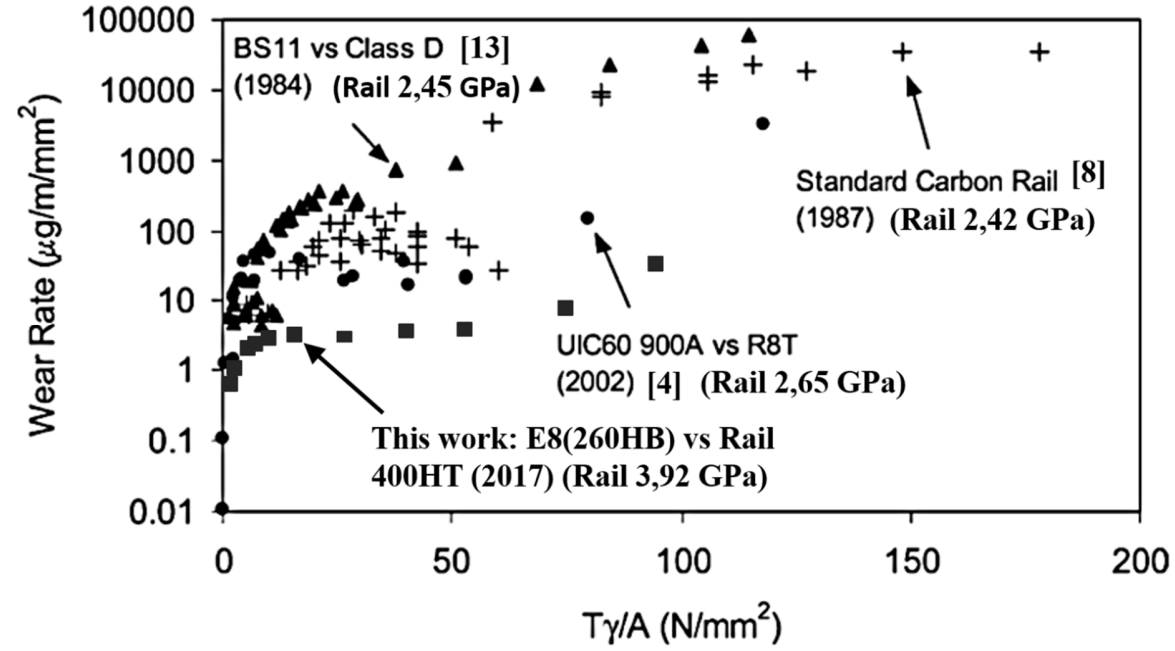


(a)

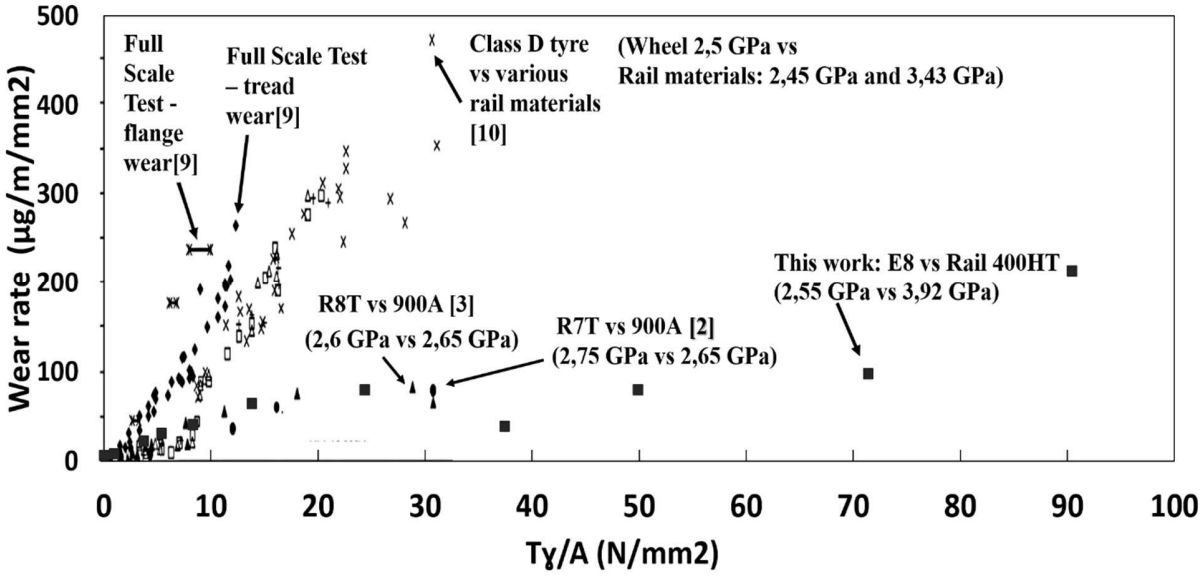


(b)

***Figure 5 .*** *Comparison of wear rates of R400HT rail steel (a) and E8 wheel steel (b) with reports from the*

*literature for several wheel-rail material pairs. Figures adapted from [4] and [2] respectively with new data added.*

**Fig. 6** shows the typical aspect of the worn surface of rail and wheel samples after the twin disc tests with 1%, 5% and 10% slip ratio. Damage in rail samples proceeds mainly by ratchetting and surface cracking, while in wheel samples spalling and adhesive wear are the predominant mechanisms.

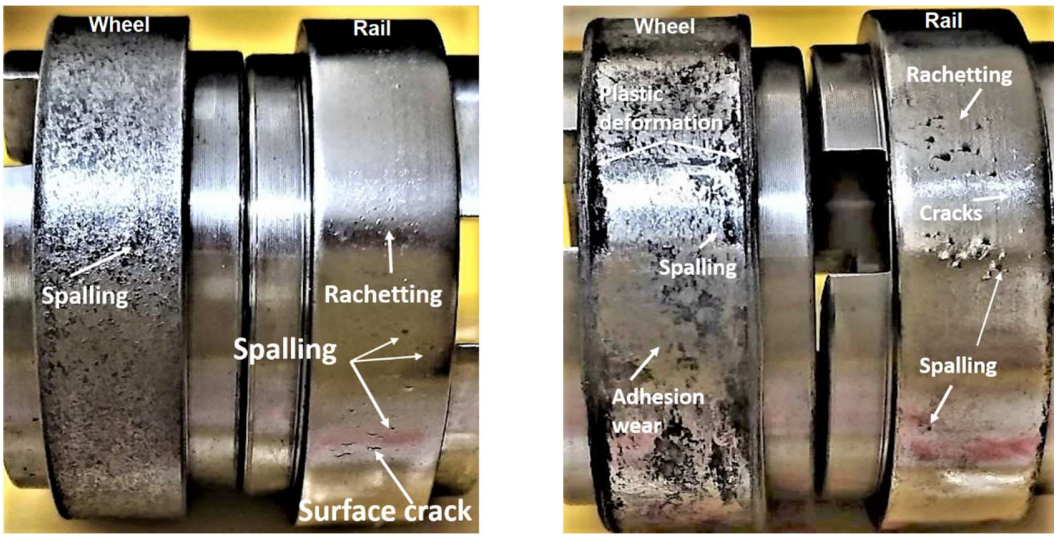


a) 1% slip

b) 5% slip

c) 10% slip

***Figure 6.*** *Aspect of the worn surface of wheel and rail samples after twin disc tests with different slip ratios.*

**Fig. 7** presents SEM images of the worn surface and light optical microscope (LOM) images of the cross section of rail samples after tests with slip ratios of 1%, 5%, and 10%. Ratchetting marks and small surface cracks are evident in samples tested with 1% slip ratio, in which the mean angle of propagation of the cracks with respect to the surface is circa 5°. After the tests with 5% slip ratio the ratchetting marks become larger and the overall damage of the surface is more intense, while for 10% slip ratio the amount and size of the wear marks reduce again, and the surface is somehow similar to that observed after the tests with 1% slip ratio.

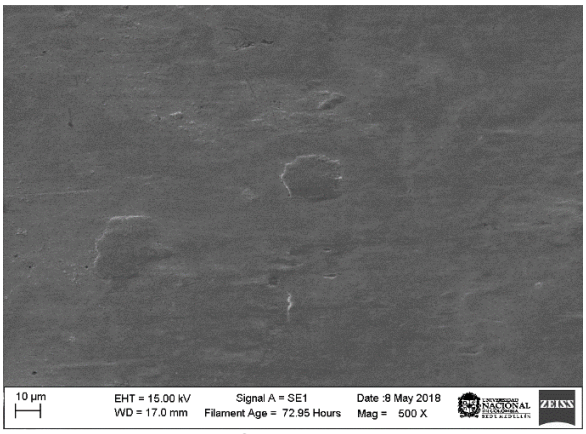


a) Slip ratio 1%

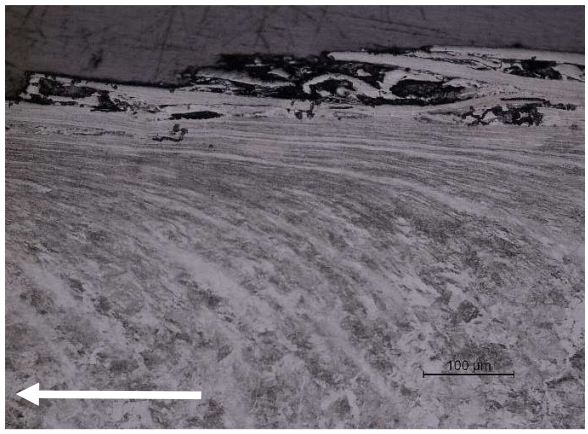


b) Transverse section 1%

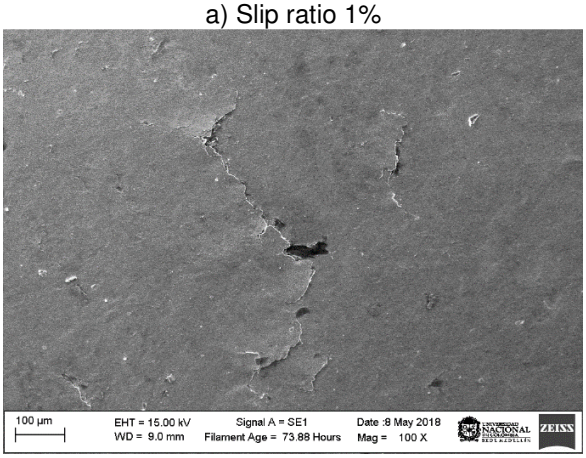


c) Slip ratio 5%

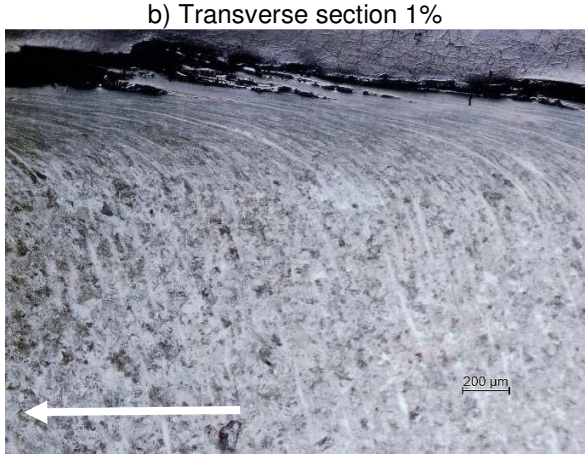


d) Transverse section 5%

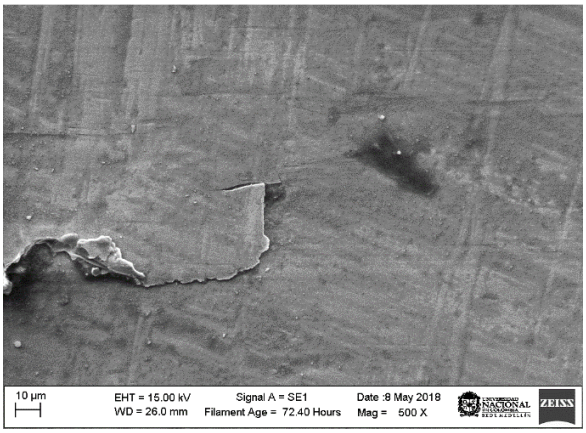


e) Slip ratio 10%

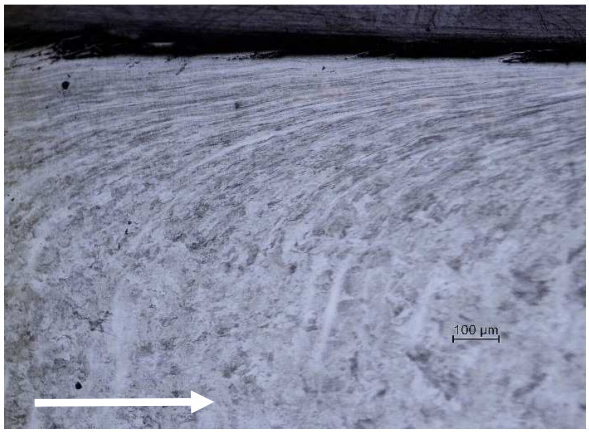


f) Transverse section 10%

***Figure 7.*** *Aspect of the worn surface (SEM: a, c, e) and cross-section (LOM: b, d, f) of premium R400HT rail after twin-disc tests with different slip ratios. The arrows on cross-sections (b, d, f) show the rolling directions.*

The crack angle increases with the slip ratio to a value around 12° for slip ratio 10% as shown in **Fig. 8**, in which it can also be seen that the depth of the deformed layer reaches a maximum of 365 µm at 5% slip ratio and then decreases to circa one third of that value at 20% slip ratio. These results are consistent with the observed variation of microhardness with the distance from the surface as illustrated in **Fig. 9**. Changing the slip ratio from 1% to 5% causes a significant increase in the hardness near the contact surface as well as in the depth of the hardened layer. On the other hand, when the slip ratio increases to 10% the depth of the hardened layer is just slightly larger than that observed for a slip ratio of 1%. Further increases in slip ratio lead to a softer surface despite the strain hardening process being more intense for larger slip ratios. This is caused by the removal of external, harder layers, of material due to sliding friction, leaving sub-surface, softer layers, as “new” surfaces.

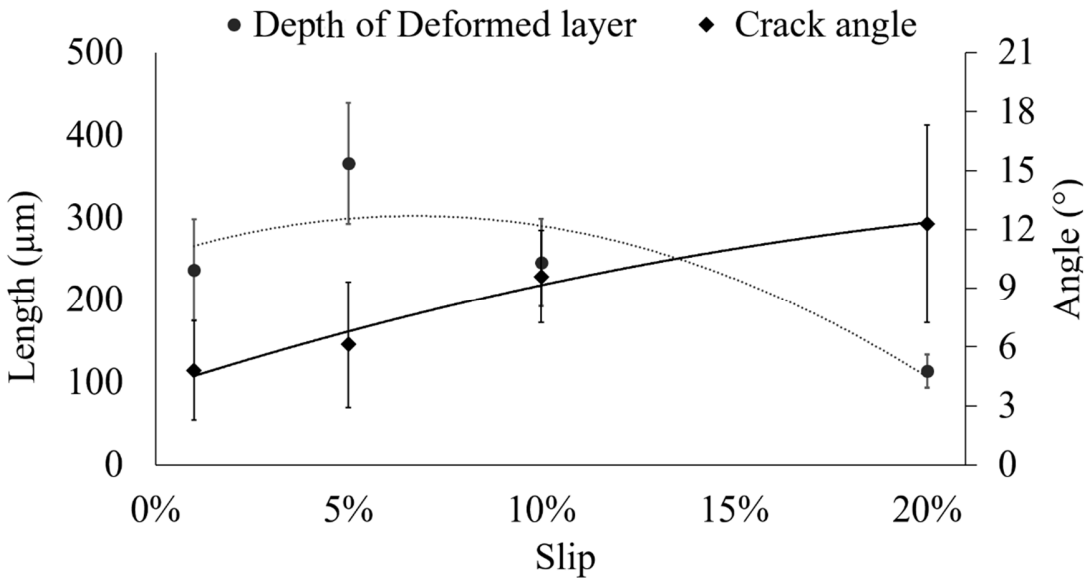


***Figure 8.*** *Variation of mean crack angle with respect to the surface and depth of deformed layer as a function of the slip ratio for premium R400HT rail.*

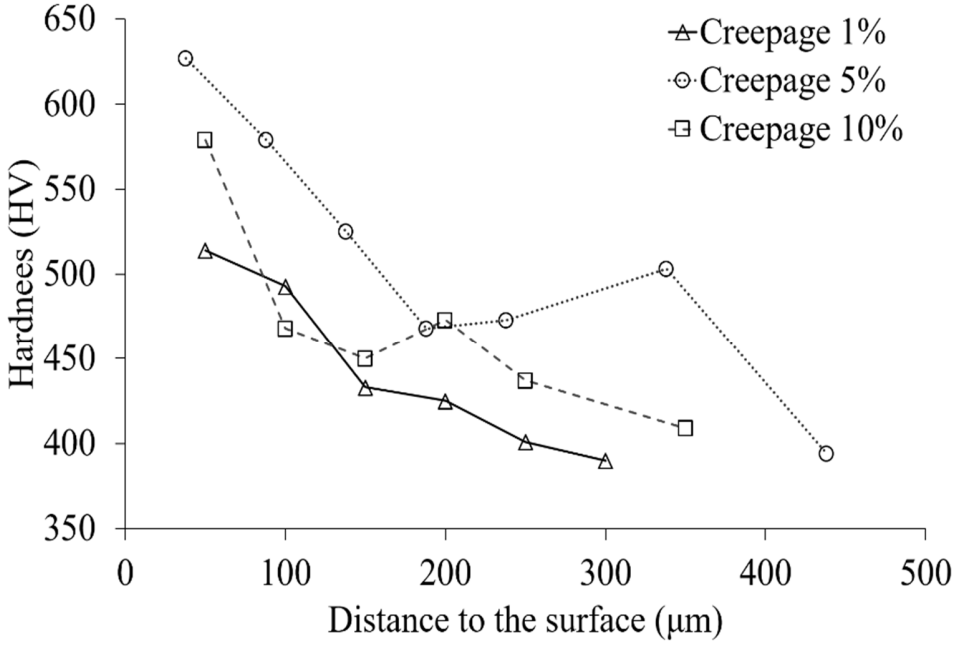


***Figure 9.*** *Variation of microhardness of premium R400HT rail as a function of the distance from the worn surface for three different slip ratios.*

### 3.2 RCF behaviour

The results of mass losses of the three rail steels with two replicas after wear tests performed up to 20 thousand (20k) cycles (8k dry cycles and 12k wet cycles) are shown in **Fig. 10**. Generally speaking, when the hardness (H) of the rail is higher the wear rates (WR) are lower.

When rolling contact fatigue is induced by pressurization using water, the lowest mass loss was found for the hardened R400HT rail. The highest mass losses were found for the standard R260 rail for which the wear rate was around 4 times higher than in R400HT rail. The coefficient of friction for the test rails (not shown) was very similar for all the tested pairs although slightly lower values were found for the softer rails. **Fig. 10** also shows the wear rates under dry conditions (after 8k cycles). From the data the same trend (lower wear of the rail material for higher hardness) was observed, with the wear rate under dry conditions for the standard rail (R260) being around 2 times higher than that for the hardest rail (R400HT).

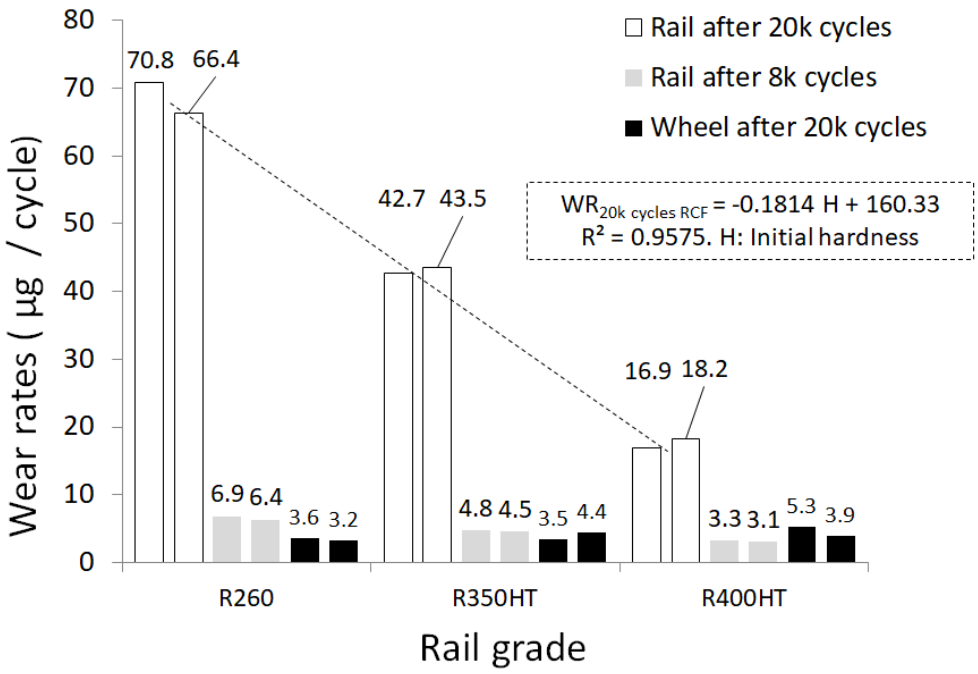


**Figure 10.** *Wear rates after dry and wet tests with different rail materials*

An issue that has been discussed by maintenance engineers is if the use of hardened rails will affect the behaviour and/or cause high wear rates in the wheels. **Fig. 10** also shows that the wear rates of wheels after 8k dry then 12k wet cycles were higher when the hardened R400HT was used. Results obtained by the manufacturer of premium rails in Full-Scale Rig (FSR) tests [26] showed that the wear rates of the wheels rolling against different rails were very similar. However, these results were obtained under dry rolling-sliding after 100k wheel passes (cycles). The damage caused by shelling in the twin-disc test can affect the results since the debris from the rail (detached shells) can cause abrasion on the surface of the wheel samples. This clearly has to be considered since it does not represent the conditions in the field.

**Fig. 11** shows the worn surfaces of the samples after the 20k cycles of testing. The damage was different for every rail and the largest flakes were found for the R260 rail. The same figure also shows the deformed layers after rolling-sliding for 8k dry cycles. The white arrows at the bottom-right show the rolling-sliding directions. The thickness of the deformed layer varied from 60 to 160 μm for the different rail materials. The deepest deformed layer was found for the R260 rail, while the shallowest one was found for the R400HT rail. Similar to what was found for the hardness, there is a linear relation between the thickness of the deformed layer (t) in μm and the wear rate (WR) during the test.

a) R260 b) R350HT c) R400HT

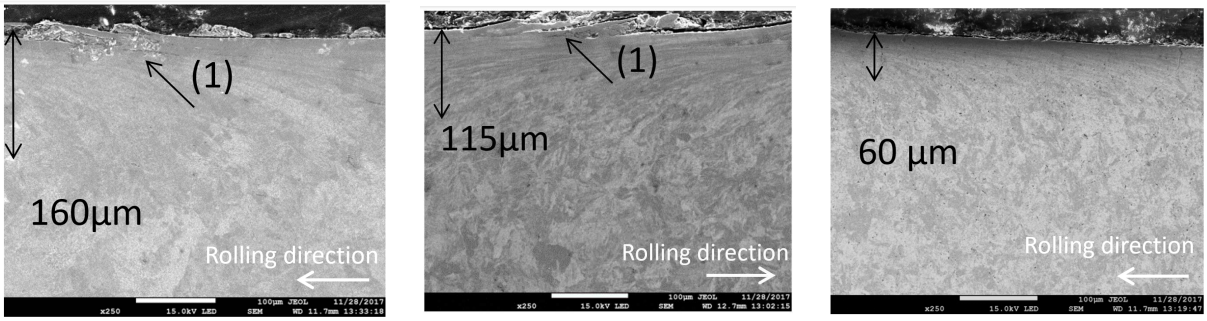


d) Transverse section R260 **e)** Transverse section R350HT f) Transverse section R400HT

***Figure 11.*** *Worn surfaces of the samples after the tests*

**Fig. 12** shows the initial and final hardness after 8k dry cycles, as well as the thickness of the deformed layer for the three rail materials studied. The difference between the final and initial hardness shows that even harden rails can be strain-hardened during rolling-sliding tests. **Fig 12** also shows the depth of the cracks for the different rail materials and the spacing between them. The cracks were shallower for the hardened rail (R400HT) while the deepest cracks were found for the standard rail material (R260). A closer inspection of the samples after the full 20k cycles showed cracks with lengths ranging from 153 µm to 730 µm with mean angles from 8° to 23°. The density of cracks was higher for the softer rail.

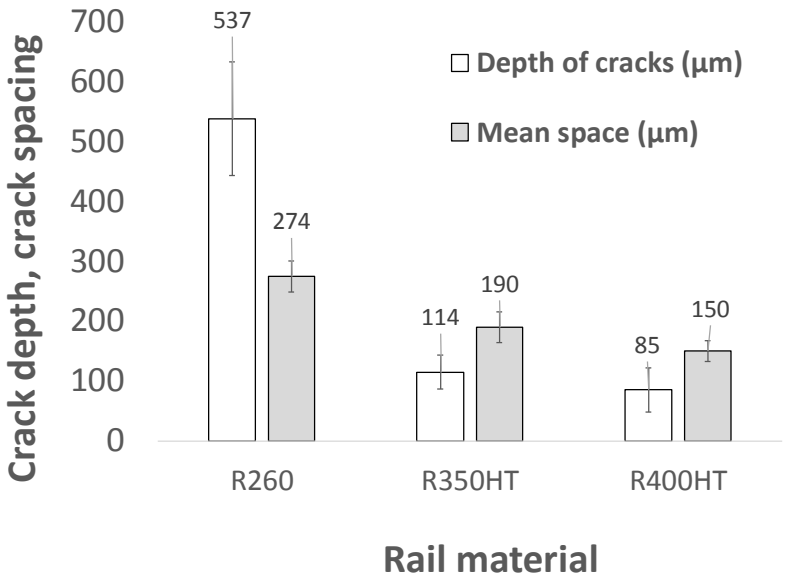


a) Initial and final hardness after 8k dry cycles and thickness of the deformed

layer.

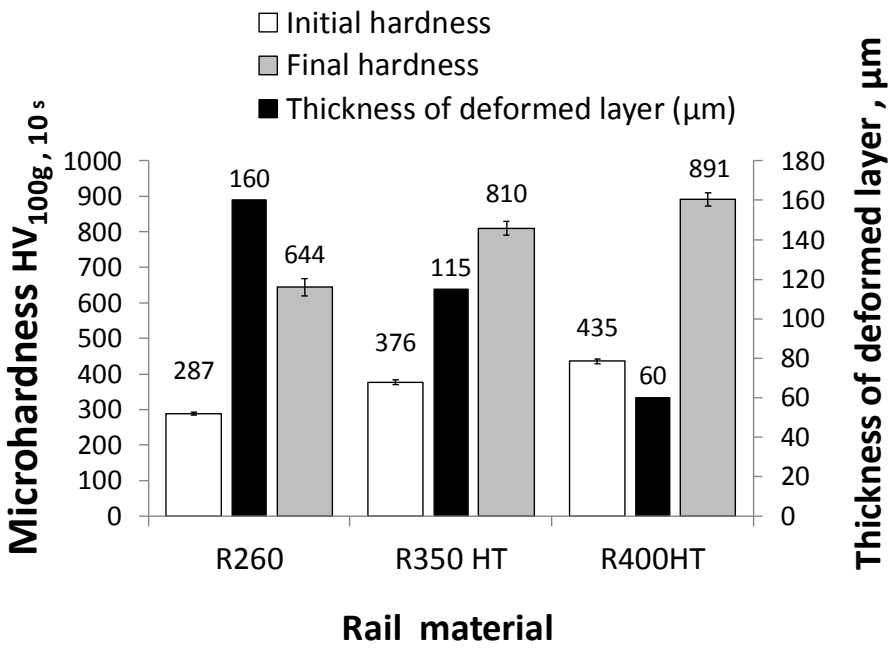


b) Maximum cracks depth and mean space between cracks in the discs after 20k cycles

***Figure 12.*** *Results from rolling contact fatigue tests*

Regarding the difference between the cracks in the standard and the hardened rail, Németh [27] found that, for similar operating conditions in the field, the mean distance between cracks was different for different rail materials: the number of cracks per unit length was typically higher in hardened rail than in standard rail. In the current laboratory study, the mean crack spacing in the samples was also measured and the grey bars in **Fig. 12b** show the results. It is observed that hardened rails have a lower mean crack spacing than standard rails. However, even though there are more cracks per unit length, the cracks are shallower and consequently the removal of material induced by RCF is lower than that observed for standard R260 rail. Stock and Pippan [19] studied the influence of rail grade on surface damage using a Full-Scale Rig and found trends for the variation of the depth of plastic deformation and the surface crack spacing in the same three rails studied in this work. Their results are similar to what is presented in Figs. 11 and 12, i.e. both the size of the plastically deformed zone and the mean surface crack spacing decrease with hardness. However, the mentioned authors found that the ratio between the

surface crack spacing and the depth of plastic deformation was practically a fixed value regardless the rail grade, with a value of approximately 2. In the current work, on the other hand, this value was similar for R260 and R350HT grades (1.71 and 1.65, respectively) but significantly higher for R400HT (2.50). Further analyses are needed to uncover the reasons behind this discrepancy, but it seems reasonable to relate them to intrinsic differences between the Full-scale and the twin-disc tests.

### 3.3 Overall comparison of hardened and standard rails

Nowadays, premium hardened rails are commonly used in transportation systems. For instance, Metro de Medellín (who kindly provided the materials for this research) use hardened rails such as R350HT and R400HT in about 40 curves of its commercial line. The Tgamma data obtained in this article for premium rails (R400HT) rolling-sliding against typical wheels may be useful to researchers who simulate the contact between wheel and rail to predict the development of wheel and rail profiles. Those simulations use Tgamma relations to predict the loss of profile (see for example refs [12] and [25]). The data reported in the literature and the results described in this article are summarized in **Table 2**. For intermediate values of Tgamma several authors have found that the wear rates do not depend on the Tgamma value and consequently they are fixed. If that value is compared for hardened rails (around 10 μg/m mm²) and standard rail (around 55 μg/m mm²), it is clearly suggested that the use of hardened rails will result in less wear at the interface. Of course, more data is required to validate this conclusion for other types of hardened rails.

On the other hand, the results of accelerated RCF tests showed that hardened rails are more resistant to contact fatigue than standard rails. This agrees with the results provided by other studies [24, 26]. However, the same result was not found in the field, and cracks appeared at the surface of a hardened premium rail R400HT just a few months (8 MGT of vehicles) after installation in the Metro de Medellín's commercial line [22]. This implies that there is at least one variable in the field that is not being properly simulated in the laboratory with the twin-disc tests. Even though the RCF resistance of the premium rail material is higher, it can be affected by in the field by the railway operator and/or by systemic factors such

as ballast consolidation, vehicle parameters, among others. In this case, before the installation of the R400HT rail in the field, a grinding operation must be performed to obtain a proper rail profile. The contradictory results from the lab and the field may indicate that the grinding operation can alter the expected RCF behaviour of the rails. This topic is currently under research and the results of the analysis will be presented in a future work.

**Table 2.** Wear prediction obtained from Tgamma approaches for R260 and R400HT

| **Source** | **Rail material** | **Wheel material** | **Wear equation** | **Tɣ (N) or Tɣ/A (N/mm²)** | **Wear rates (D diameter of wheel in mm)** |
|---|---|---|---|---|---|
| Pearce and Sherratt [12] | BS11 | R8T | Wheel | Tɣ < 100 | 0.25 Tɣ/D [mm²/km] |
| Pearce and Sherratt [12] | BS11 | R8T | Wheel | 100 ≤ Tɣ < 200 | 25/D [mm²/km] |
| Pearce and Sherratt [12] | BS11 | R8T | Wheel | Tɣ ≥ 200 | (1.19 Tɣ - 154)/D [mm²/km] |
| Lewis et al [25] | 900A | R8T | Wheel | Tɣ/A < 10.4 | 5.3Tɣ/A [µg/m mm$^2$] |
| Lewis et al [25] | 900A | R8T | Wheel | 10.4 < Tɣ/A < 77.2 | 55 [µg/m mm$^2$] |
| Lewis et al [25] | 900A | R8T | Wheel | Tɣ/A > 77.2 | 61.9 Tɣ/A [µg/m mm$^2$] |
| This work | R400HT | E8 | Wheel | Tɣ/A ≤ 25 | 3.16 Tɣ/A [µg/m mm$^2$] |
| This work | R400HT | E8 | Rail | Tɣ/A ≤ 25 | 0.87 Tɣ/A [µg/m mm$^2$] |
| This work | R400HT | E8 | Rail | 25 ≤ Tɣ/A < 70 | 10 [µg/m mm$^2$] |

## 4. CONCLUSIONS

The wear rates of premium R400HT rail and E8 wheel samples were determined as a function of the energy provided to the contact interface in laboratory twin-disc tests. An initial contact regime was observed in which the wear rate increased linearly with the wear index *Tγ/A* for both wheel and rail samples. A second stage, characterized by the independence of the wear rate and wear index, was also easily identified, with a stable wear rate for the rail samples approximately one order of magnitude lower than that of the wheel samples. For very high slip values, considerable damage at the surfaces was observed, which is consistent with a second regime transition to a catastrophic condition.

The wear rates of both R400HT rail and E8 wheel materials measured in twin disc tests were systematically lower than those reported by other researchers in tests performed with softer rail materials. The threshold values of the wear index $T\gamma/A$ related to wear regime transitions were also lower when the hardened rail material was used.

Laboratory testing was performed to assess rolling contact fatigue of different rails with pre-existing RCF cracks. The application of water caused accelerated crack growth and the method allowed significant differences between different rail materials to be identified. The lowest mass losses were found for the hardened R400HT rail. The highest mass losses were found for standard R260 rail. Higher hardness was associated with a lower wear rate.

The thickness of deformed layers was found to vary from 60 to 255 μm for the different rail materials while the cracks lengths ranged from 153 μm to 730 μm with a mean angle from 8° to 23°. The largest deformed layer and highest crack density were found for the R260 rail while the smallest ones were found for the R400HT rail. Also, there was a correlation between the thickness of the deformed layer and the mass losses found during the tests.

**Acknowledgments**

The authors are grateful to the Royal Academy of Engineering for financial support through the Industry Academia Partnership Programme, project n. IAPP\1516\91, and to the Metro de Medellín for providing rails and wheels for study, as well as for facilitating the access for field inspections.

**References**

[1] M. Hiensch, M. Steenbergen, Rolling Contact Fatigue on premium rail grades: Damage function development from field data, Wear 394–395 (2018) 187–194.

[2] R. Lewis, R.S. Dwyer-Joyce, U. Olofsson, J. Pombo, J. Ambrósio, M. Pereira, C. Ariaudo, N. Kuka, Mapping railway wheel material wear mechanisms and transitions, Proc. Inst. Mech. Eng. Part F J. Rail Rapid Transit 224(3) (2010)125–137.

[3] R. Lewis, R.S. Dwyer-Joyce, Wear mechanisms and transitions in railway wheel steels, Proc. IMechE, Part J: Engineering Tribology 218 (2004) 467–478.

[4] R. Lewis, U. Olofsson, Mapping rail wear regimes and transitions, Wear 257(2004) 721–729.

[5] U. Olofsson, T. Telliskivi, Wear, friction and plastic deformation of two rail steels - full-scale test and laboratory study, Wear 254 (2003) 80–93.

[6] E. Sheinman, Wear of Rails. A Review of the American Press, Journal of Friction and Wear 33(4) (2012) 308-314.

[7] U. Olofsson, R. Nilsson, Surface cracks and wear of rail: a full-scale test and laboratory study, Proc. IMechE Part F J. Rail Rapid Transit 216 (2002) 249–264.

[8] D. Danks, P. Clayton, Comparison of the wear process for eutectoid rail steels: field and laboratory tests, Wear 120 (1987) 233–250.

[9] I.J. McEwen, R.F. Harvey, Full-scale wheel-on-rail testing: comparisons with service wear and a developing theoretical predictive model, Lubr. Eng. 41(2) (1985) 80–88.

[10] P.J. Bolton, P. Clayton, Rolling-siding wear damage in rail and tyre steels, Wear 93 (1984) 145–165.

[11] L. Ma, C.G. He, X.J. Zhao, J. Guo, Y. Zhu, W.J. Wang, Q.Y. Liu, X.S. Jin, Study on wear and rolling contact fatigue behaviors of wheel/rail materials under different slip ratio conditions, Wear 366-367 (2016) 13–26.

[12] T.G. Pearce, N.D. Sherratt, Prediction of wheel profile wear, Wear 144 (1991) 343–351.

[13] T. Jendel, Prediction of wheel profile wear—methodology and verification, Licentiate Thesis, TRITA-FKT 2000:9, Royal Institute of Technology, Stockholm, Sweden, 2000.

[14] M. Kaneta, Y. Murakami, Effects of oil hydraulic pressure on surface crack growth in rolling/sliding contact, Tribology international 20(4) (1987) 210-217.

[15] A.F. Bower, The Influence of Crack Face Friction and Trapped Fluid on Surface Initiated Rolling Contact Fatigue Cracks, J. Tribol. 110 (1988) 704–711.

[16] W.R. Tyfour, J.H. Beynon, A. Kapoor, The steady state wear behaviour of pearlitic rail steel under dry rolling-sliding contact conditions, Wear 180 (1995) 79-89.

[17] D.I. Fletcher, J.H. Beynon, The influence of lubricant type on rolling contact fatigue of pearlitic rail steel, Tribology Series 36 (1999) 299-310.

[18] Q. Liu, W. Jiang, E. Magel, Study of rolling contact damage function by twin-disk test, In: Proceedings of the 9th International Conference on Contact Mechanics and Wear of Rail/Wheel Systems (CM2012), Chengdu, China, Aug 27-30, 2012.

[19] R. Stock, R. Pippan, Rail grade dependent damage behaviour–Characteristics and damage formation hypothesis, Wear, 314(1-2) (2014) 44-50.

[20] D.T. Eadie, D. Elvidge, K. Oldknow, R. Stock, P. Pointner, J. Kalousek, P. Klauser, The effects of top of rail friction modifier on wear and rolling contact fatigue: Full-scale rail–wheel test rig evaluation, analysis and modelling, Wear 265(9-10) (2008) 1222-1230.

[21] J.F. Santa, P. Christoforou, P.A. Cuervo, A. Toro, A. Beagles, R. Lewis, Evaluation of rolling contact fatigue of rail materials in twin disc tests. Proceedings of the 11th international conference on contact mechanics and wear of rail/wheel systems (CM2018), Delft, The Netherlands, September 24-27, 2018, p 838-843.

[22] P. Cuervo, P. Christoforou, R. Lewis, A. Beagles, J.F. Santa, A. Toro, Twin-disc assessment of wear regime transitions in R400HT– E8 pairs. Proceedings of the 11th international conference on contact mechanics and wear of rail/wheel systems (CM2018), Delft, The Netherlands, September 24-27, 2018. P181-188

[23] Internal report. Metro de Medellín to National University of Colombia. Inspection of R400 HT rails in the field, 2017.

[24] C. Hardwick, R. Lewis, R. Stock, The effects of friction management materials on rail with pre-existing RCF surface damage, Wear 384 (2017) 50-60.

[25] J.F. Santa, Development of a lubrication system for wear and friction control in wheel/rail interfaces. PhD Thesis, National University of Colombia, Medellín, Colombia, 2012.

[26] R. Lewis, F. Braghin, A. Ward, A S. Bruni, R.S. Dwyer-Joyce, K. Bel Knani, P. Bologna, Integrating Dynamics and Wear Modelling to Predict Railway Wheel Profile Evolution. In: Ekberg, A., Kabo, E.

and Ringsberg, J., (eds.) 6th International Conference on Contact Mechanics and Wear of Rail/Wheel Systems: CM2003, Gothenburg, Sweden, June 10-13, 2003, pp. 7-16. ISBN 9163139286

[27] Private communication. Vostalpine to Metro de Medellín. Inspection of R400 HT rails in the field 2017.

[28] Németh, A. Case studies in railway construction rolling contact fatigue rail defects. Széchenyi István University. Available online in:

http://www.sze.hu/~fischersz/Education/Case%20studies%20in%20railway%20construction/CSRC_Topic%2008_Rolling%20contact%20fatigue%20rail%20defects.pdf. Last visit: July 2018